Journal of Arid Environments 83 (2012) 86–93

Contents lists available at SciVerse ScienceDirect

Journal of Arid Environments

journal homepage: www.elsevier.com/locate/jaridenv

Seasonal dynamics of vegetation over the past 100 years inferred from tree rings and climate in Hulunbei'er steppe, northern China

Z.-J. Chen [a], J.-B. Li [b,c], K.-Y. Fang [d], N.K. Davi [b], X.-Y. He [a,e,*], M.-X. Cui [a], X.-L. Zhang [a], J.-J. Peng [a]

[a] State Key Laboratory of Forest and Soil Ecology, Institute of Applied Ecology, Chinese Academy of Sciences, 72 Wenhua Road, Shenyang 110164, PR China
[b] Tree-Ring Laboratory, Lamont-Doherty Earth Observatory, Columbia University, NY 10964, USA
[c] International Pacific Research Center, University of Hawaii at Manoa, Honolulu, HI 96815, USA
[d] MOE Key Laboratory of Western China's Environmental Systems, Lanzhou University, Lanzhou 730000, PR China
[e] Northeast Institute of Geography and Agroecology, Chinese Academy of Sciences, Changchun 130012, PR China

ARTICLE INFO

Article history:
Received 3 January 2010
Received in revised form
18 May 2011
Accepted 22 March 2012
Available online xxx

Keywords:
NDVI
Moisture variability
Mongolian pine
Reconstruction
Semi-arid grassland
Tree-ring width

ABSTRACT

The relationship between monthly vegetation cover anomalies and climate in the Hulunbei'er steppe were studied through analyzing the relationship between regional normalized difference vegetation index (NDVI) and climatic variables, and NDVI and tree-ring width during the growing season (May–October). The local moisture (dry/wet) and temperature (cold/warm) variations largely affected the vegetation cover and the radial growth of Mongolian pines (*Pinus sylvestiris* Linnaeus var. *mongolica* Litvinov) in the steppe. Monthly precipitation and Palmer drought severity index (PDSI) data from the previous to the current growing seasons were positively correlated to regional vegetation cover and radial growth of Mongolian pines; however, negative correlations were found between temperature and vegetation variables. A reconstruction of monthly vegetation cover dynamics for the growing season was created and spans 116 years (from 1891 to 2006). The results show that the total numbers of anomalies for dense and sparse seasonal vegetation cover is 22 years over the 116 year record; about 5–7 relatively dense or sparse periods; and ~2–8 years significant periodicities ($p < 0.05$). Linkages to the Pacific Ocean and Arctic Ocean regimes were also detected.

1. Introduction

Temperate grasslands are one of the most widespread biomes on earth and play an important role in regional ecosystem dynamics (Ma et al., 2008; Scurlock et al., 2002). In China, natural grasslands cover 393 million hectares, making up approximately 41.7% of national territory (2005 Report on the State of the Environment in China, State Environmental Protection Administration). Grasslands extend 4500 km from the Northeast China Plain, through the Inner Mongolia Plateau and the Loess Plateau to the Tibet Plateau (Li, 1999; Ma et al., 2008). Our study area named Hulunbei'er steppe, is a typical grassland that offers a wonderful grazing pasture due to its high palatability of herbs and high quality and quantity of herb production and is a region that has been grazed by nomadic herds for centuries. Many local people, livestock and wild animals are influenced by changes in the vegetation condition (dense and sparse). The density of vegetation cover in the grasslands has also been associated with dry/wet and cold/warm climate variability (Fabricante et al., 2009, Fang et al., 2005; Jiang et al., 2006; Ma et al., 2008; Schultz and Halpert, 1993; Yi, 2003). Recent intensified grazing pressure and sedentary agricultural practices has led to an increase in soil erosion and desertification, decreasing the grassland quality and productivity (Jiang et al., 2006; Wang, 2004; Zhang and Liu, 1992). However, the grassland still remains natural overall, and climate is a dominant controlling factor for vegetation succession (Han, 2001; Ma et al., 2008; Yi, 2003).

Instrumental and historical vegetation records around the world are very limited prior to the 1980s, particularly at the remote inland grassland region of China. Quantitative information about long-term vegetation variability is especially valuable for eco-environmental and socioeconomic studies, particularly in relatively pristine pasturing areas. Therefore, long-term records of vegetation cover and an enhanced understanding of the regional environmental and social change are necessary for the steppe.

NDVI is an ideal indicator of vegetation biomass activity, and parameters such as temperature, precipitation and other climatic

* Corresponding author. State Key Laboratory of Forest and Soil Ecology, Institute of Applied Ecology, Chinese Academy of Sciences, 72 Wenhua Road, Shenyang 110164, PR China. Tel.: +86 24 83970349; fax: +86 24 83970300.
E-mail address: hexy@iae.ac.cn (X.-Y. He).

0140-1963/$ – see front matter © 2012 Published by Elsevier Ltd.
doi:10.1016/j.jaridenv.2012.03.013

variables are necessary to explain the variance exhibited by the NDVI (Schultz and Halpert, 1993; Tucker, 1979, Tucker et al., 2004). More recently, NDVI has been used in climate and biogeochemical models to calculate photosynthesis, the exchange of CO_2 between the atmosphere and the land surface, land surface evapotranspiration, and the absorption and release of energy by the land surface. Many studies involving comparisons between climatic variables, tree rings and NDVI have been carried out at different spatial and temporal scales (He and Shao, 2006; Kaufmann et al., 2004; Liang et al., 2005; Wang et al., 2004). In China, NDVI has also been used to detect changes in phenology, to retrieve land vegetation cover, to classify vegetation on a large scale, to estimate vegetation biomass and net primary productivity, or to indicate vegetation's responses to climate change as well as its feedback (He and Shao, 2006).

The objectives of the present study are: (1) to identify whether synthesized climatic variables, such as PDSI can reflect NDVI in the steppe; (2) to reconstruct past variations of grassland biomass using NDVI; (3) to discuss past vegetation dynamics in the arid and semi-arid steppe in terms of regional dry/wet and cold/warm climate conditions; and (4) to indicate which climatic parameters are appropriate indicators of vegetation variability and can be used as reliable predictors of vegetation change.

2. Materials and methods

2.1. Study area and climate

The Hulunbei'er steppe is located in northern China (47°20′ ~ 50°13′N; 115°31′ ~ 121°10′E; altitude: 650–700 m a.s.l., Area: 93,000 km^2, Appendix Fig. 1). It is one of the most important rangeland regions in northern China due to its large and high quality pastures (Zhang and Liu, 1992), which are dominated by perennial and annual grasses (Wang, 2004). The study region is characterized by a typical continental monsoon climate with limited precipitation and air humidity (Yang et al., 1992). It is semi-arid or arid to the west of the steppe, with temperature and precipitation decreasing gradually and the landscape transitioning from steppe, to semidesert, to desert or Gobi respectively from east to west. East of the steppe, neighboring the Great Xing'an Mountains, there is a temperate climate with increasing precipitation and warming temperatures, and temperate mixed forests and flood plain dominating the landscape. The regional mean annual temperature and total precipitation are respectively ~0.2 °C and ~270 mm (a rainfall profile of ~250–~500 mm indicates the typical semi-arid area in China). The maximum regional difference of annual mean temperature and annual total precipitation are ~1.8 °C and ~70 mm, respectively. The snowpack usually occurs from October to April, but sometimes from September to May. The amount of melting water accounts for 7.32%–16.53% of the annual total precipitation. The July–August (summer) precipitation accounts for 55.97% of the annual total precipitation (Appendix Fig. 2A).

2.2. NDVI and PDSI

NDVI is the ratio between near-infrared (NIR, from 0.7 to 1.1 μm) and visible (VIS, from 0.4 to 0.7 μm) and red (RED, from 0.6 to 0.7 μm) portions of the electromagnetic spectrum, which can be calculated as NDVI = (NIR − RED)/(NIR + RED) (Tucker, 1979). According to the definition, the NDVI itself varies between −1.0 and +1.0, ranging from 0.05 for sparse vegetation to 0.7 for dense vegetation cover (Tucker and Sellers, 1986). NDVI data over the entire globe from NASA and NOAA (Global Land Cover Facility, www.landcover.org) are used to explore plant productivity in the study region and its relationships to regional climatic change. The dataset is derived from imagery obtained from the Advanced Very High Resolution Radiometer instrument onboard the NOAA satellite series to provide a 22 year 8 km × 8 km resolution satellite record of monthly changes in terrestrial vegetation. The new features of this dataset include reduced NDVI variations arising from calibration, view geometry, volcanic aerosols, and other effects not related to actual vegetation change (Tucker et al., 2004). The study area (48° ~ 50°N, 115° ~ 120°E) covers almost the entire grassland of Hulunbei'er in northern China (Appendix Fig. 1A).

PDSI is a meteorological drought metric based upon a water balance model in which temperature, precipitation and soil characteristics are considered (Palmer, 1965), whereby positive and negative PDSI values correspond to wet and dry conditions respectively. Typical values of PDSI range from a minimum of −4.0 (severe drought) to a maximum value of 4.0 (very wet), with 0.0 ± 0.5 indicating "normal" moisture conditions. The current commonly used 2.5 × 2.5 gridded PDSI series (Dai et al., 2004) consist on monthly PDSI over global land areas from 1870 to 2003 (updated to 2005 on November 7, 2006). The PDSI is calculated using monthly surface air temperature (from Jones and Moberg, 2003 and updates) and precipitation data (from Dai et al., 1997 before 1948 and Chen et al., 2002 from 1948 to present). Since there are relative few meteorological stations in the region beginning before 1950, we consider the PDSI data post 1950 more reliable than the 1894–1949 period. After comparison of several girds, we selected the data from the grid located at 48°45′N, 118°45′E, which is near to more meteorological records in the area, in order to detect regional environmental variations.

2.3. Tree-ring data

Generally, seasonal variability of NDVI from the regional grasslands and nearby tree growth is similar, and NDVI can be simulated by tree-ring records (He and Shao, 2006; Kaufmann et al., 2004; Liang et al., 2005). Thus, the regional NDVI data were compared with nearby tree-ring width data to verify the validity and consistency of the annual growth rings with dynamic changes of regional vegetation.

The regional dominant tree species, Mongolian pine, is located on scattered sand dunes along the eastern boundary of the semi-arid and arid steppe (48°8′N ~ 48°16′N, 119°48′E ~ 119°59′E, 720–870 m a.s.l.) (Appendix Fig. 1). One or two cores per tree were sampled from different directions at breast height. In total twenty-five increment cores from 15 living trees were extracted using an increment borer. Conventional dendrochronological techniques (Cook, 1985; Fritts, 1976; Holmes, 1983) were used in developing the ring width chronologies. The samples were mounted, air dried and sanded (Stokes and Smiley, 1968). Tree rings were crossdated visually, and measured with a LINTAB5 measuring system with a resolution of 0.001 mm. Subsequently, the measurements were checked by the program COFECHA for quality control (Holmes, 1983). Considering the close locations of the dune sites and their environmental homogeneity, all the measurements were merged to develop one composite ring width chronology. The crossdated raw ring widths were detrended using conservative growth curves such as negative exponential or linear curves. We also used a cubic smoothing spline (about 2/3 of the series length) in some cases when there appeared to be anomalous low-frequency trends that were different from other trees. Our goal was to remove biological growth trends while preserving variations that are likely related to climate. The tree-ring indices were averaged together to generate a standard chronology using the program ARSTAN (Cook and Holmes, 1986). The inter-series correlation (rBar) between trees, and the expressed population signal (EPS) with a threshold value of 0.85 or higher, were employed to determine the reliable period for analysis (Wigley et al., 1984).

2.4. Climate data

The instrumental meteorological records were obtained from China Meteorological Data Sharing Servicing System. Three meteorological station records [Manzhouli (MZL, 49°34′N, 117°26′E, 662 m a.s.l.), Xinba'erhuyouqi (XYQ, 48°40′N, 116°49′E, 554 m a.s.l.) and Xinba'erhuzuoqi (XZQ, 48°13′N, 118°16′E, 642 m a.s.l.)] were chosen to detect regional climatic signals (Appendix Fig. 1A). The meteorological stations are located at approximately the same altitude as the tree-ring sampling sites. Although the distances between these stations are relatively far (~110–160 km), significant correlations were found between all records ($p < 0.05$) (Appendix Table 1A), indicating homogeneity and coherency of regional climate during the common period of 1958–2009. Averaging meteorological records from different stations can reduce small-scale noise or stochastic components and thus improve statistical relationships between vegetation variables and meteorological data (Blasing et al., 1981; Pederson et al., 2001). Thus, the regional mean meteorological data series was developed from monthly records of the nearby stations over the common interval from 1959 to 2008. A principal component analysis (PCA) based on the correlation matrix was calculated for the common period to evaluate the shared variance of the meteorological data. The climate data used in this study include local monthly temperature, precipitation, relative humidity and duration of sunshine.

Large scale environmental variables such as East Asia Monsoon Index (EAMI) (Shi and Zhu, 2000) and El Niño-Southern Oscillation (ENSO) (http://www.esrl.noaa.gov/psd/webswitch.html) were also used in this study.

The climate-vegetation change relationships were investigated by means of correlation analyses between tree-ring data and meteorological records for their common period 1981–2001. Multi-Taper Method (MTM) of spectral analysis (Mann and Lee, 1996) was employed to examine spectral properties of these time series. To assess the influence of Pacific Ocean climate regime variability at regional-scale, we investigated the teleconnection of regional vegetation to the remote oceans.

3. Results

3.1. Regional climate variability

During the latest 50 years (1959–2008), regional mean temperatures have increased significantly by 0.040 °C/year and 0.046 °C/year for the growing season and the total year, respectively. The regional mean precipitation has decreased slightly by 0.65 mm/year and 0.49 mm/year for the growing season and the whole year, respectively, but during periods with snowpack rainfall has increased significantly by 0.14 mm/year. The regional mean humidity has decreased significantly by 0.178%/year and 0.112%/year for the growing season and the whole year, respectively. The regional annual total sunshine duration has also decreased significantly by 0.139 h/year, but the total sunshine duration during the growing season did not show clear change (decreased by 0.014 h/year). These changes indicate that the steppe has clearly experienced a drying-warming climatic process. PDSI, has decreased significantly ($p < 0.05$) during the growing season (May–October, r value of linear trend line, hereafter r_{trend}, is 0.295) and the total year ($r_{trend} = 0.319$) over the common period (1959–2005), respectively.

3.2. Chronology and tree-grass coherence

The Mongolian pine ring width chronology is 72 years in length (1936–2007). The mean EPS and rBar for 20 year intervals with 10-year overlapping are 0.901 (range from 0.858 to 0.929) and 0.286 (range from 0.210 to 0.345), respectively. In this study we only used the most reliable time span of the chronology, starting at 1947 according to the EPS criterion (EPS > 0.85).

The developed ring width chronology has high correlations with the regional NDVI data. For example, the annual mean NDVI is significantly correlated with ring width ($r = 0.710$, $p < 0.01$) over the 1981–2001 period. The high correlation is a result of the similar phenological processes; NDVI has a significant relationship with local tree growth during the growing season (May–October) (Fig. 1). The above results indicate the coherence of local vegetation change derived from satellite and actual/experimental plant growth, and thus we conclude that the NDVI data represent regional vegetation dynamics.

Based on tree rings, simple linear regression method were used to estimate seasonal and annual vegetation dynamics. The reconstructions explain a high percentage of the NDVI variance and regression model F-test (Table 1, Fig. 2). If a May–October NDVI value was in the range of its mean value (MOM) plus or minus its standard deviation (SD) during the period of 1947–2007 ($\leq$MOM $\pm$ SD$\leq$), it could be defined as a normal year of vegetation cover change, otherwise, it was labeled as a year of dense or sparse vegetation cover. According to this definition, 41 years (67.21%) were normal, 11 (18.03%) were dense and 9 (14.75%) were sparse years of vegetation cover. However, about 70% (6/9) of sparse vegetation years occurred after 1980s. MTM spectral analysis over the reliable range of tree-ring based reconstruction revealed seasonally significant spectral peaks (95% of confidence level) at ~2 years and ~4 years (Appendix Table 2), while longer than half decadal-scale cycles are not found.

3.3. Climate–NDVI change relationship

Temperature and precipitation have a clear influence on local vegetation dynamics. Generally, the vegetation cover in spring (May–June) shows a closer association with precipitation before germination, particularly the rainfall from previous summer to current spring (Appendix Fig. 3A, B). On the other hand, the vegetation cover in summer and autumn is significantly correlated with concurrent rainfall, and the growing season precipitation has a very close relationship with plant growth in July, August, September and October (Appendix Fig. 3C–F). The NDVI in May has strong negative correlations with previous June and July temperature, as well as current March and April, and it also has positive correlations with temperature from the previous October to the previous December and current May. Similar to May NDVI, June NDVI also has a significant seasonal response to temperature. The NDVI in July, August, September and October shows negative correlations with previous spring (previous summer) temperatures and positive correlations with previous winter, particularly with previous December (Appendix Fig. 3A–F).

Since the rainfall and temperature are both significantly correlated to the regional NDVI variation, the PDSI, was used to detect the NDVI responses to local dry/wet and cold/warm fluctuations. Higher correlations are found between NDVI and PDSI, compared to correlations with other single meteorological variables. The May (June) NDVI are significantly correlated to the PDSI from previous July to current May (June), respectively, and the NDVI during summer and autumn (July to October) are significantly correlated with monthly PDSI of the current growing season (May–October) (Fig. 1). Similar climate response was also found in Mongolia pine in the east boundary region of the Hulunbei'er steppe (e.g. the mean value of May–July PDSI significantly correlates with tree-ring width from 1947 to 2005, $r = 0.468$, $p < 0.01$). Seasonal climatic variables are more representative of climatic conditions during the growing season than monthly data (Cook et al., 1999). Therefore,

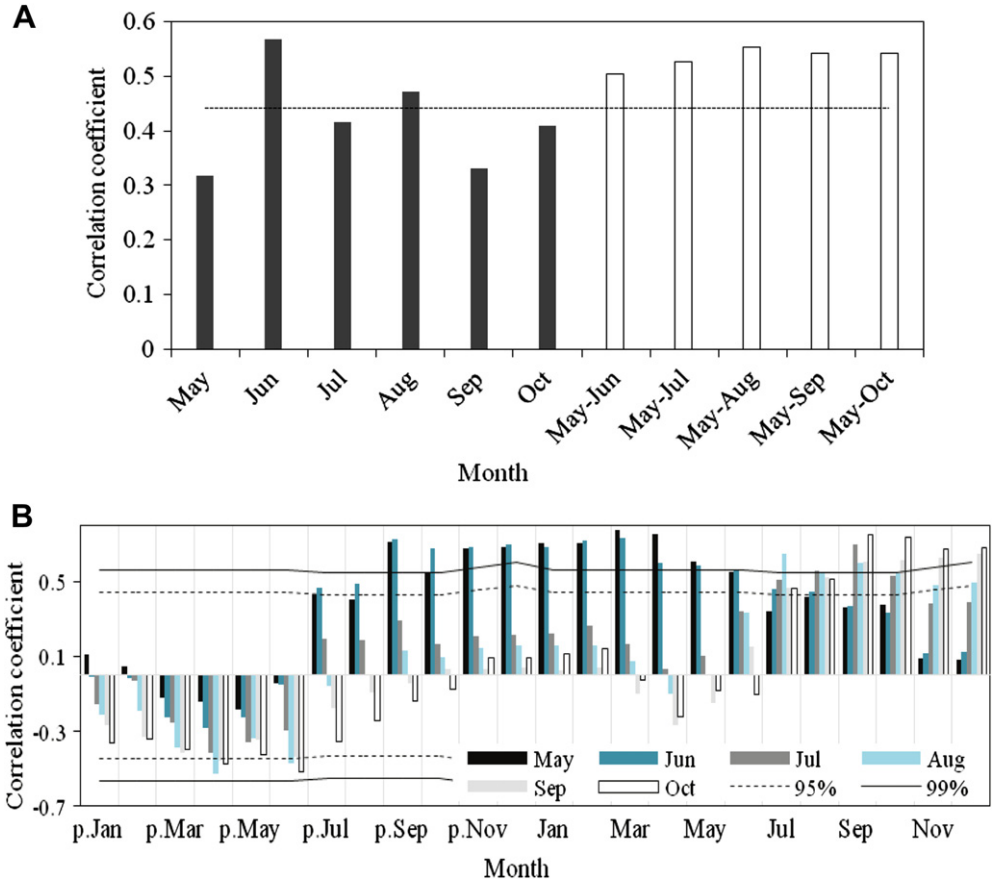

Fig. 1. (A) Correlation of tree rings and May, June (Jun), July (Jul), August (Aug), September (Sep) October (Oct) and seasonal NDVI; and (B) correlations of May, June (Jun), July (Jul), August (Aug), September (Sep) and October (Oct) NDVI with regional monthly PDSI. The black dashed lines are the 95% confidence limits and the black solid lines are the 99% confidence limits. "p." denotes the prior year.

after exploring the correlations between seasonal PDSI and NDVI, the highest correlation periods between monthly NDVI and seasonalized PDSI were used to reconstruct vegetation cover dynamics (Table 2; Fig. 3).

3.4. Monthly NDVI reconstruction and vegetation dynamics

According to the above climatic response analyses, linear regression models were built by calibrating NDVI with the monthly PDSI. During the common period 1981–2001, the regional NDVI reconstructions accounted for largest portion of the actual NDVI variance (Table 2A, Fig. 3). The statistical fidelity, such as the calibration-verification tests of the regression models, was difficult to perform due to the short length of NDVI records (20 years). Even so, the significant *F*-test results of the models demonstrate reasonable validities of these reconstructions (Table 2A). The models were built using PDSI data from various months to reconstruct regional vegetation changes, e.g. the reconstruction based on PDSI from previous July to May is for May NDVI; previous July to June PDSI is for June NDVI; July PDSI is for July NDVI; June to August PDSI is for August NDVI; July to September PDSI is for September NDVI and July to October PDSI is for October NDVI. Although some models with high explained variance show relatively low *F*-test confidence level, their results have very high coherence when they are compared with reliable regression models. Therefore, it should be considered that our selection is acceptable. The default values of the reconstructions were interpolated through regression methods for the full period (Table 2B).

Local vegetation starts to grow in May. Both actual and estimated NDVI show increasing trends until the beginning of September. The monthly increases in NDVI in May, June, July, and August are 57%, 62%, 33% and 6% than its former month, with decreases beginning in September. There are very high correlations between the monthly actual/reconstructed NDVI variables (Appendix Table 1B). In addition, the PDSI and tree-ring based May–October reconstructions show significant consistencies from 1947 to 2006 ($p < 0.05$) (Appendix Table 4).

No monthly NDVI was out of the established range; from 0.05 for sparse vegetation cover to 0.70 for dense vegetation cover (Tucker and Sellers, 1986). Over the past century the minimum monthly NDVI is 0.07 in May (1936), and maximum monthly NDVI is 0.62 in August (1902). The top 5 minimum NDVI values occur in years 1951, 1936, 1920, 2002 and 1926, respectively, and the 5 maximum NDVI years are 1955, 1910, 1929, 1984 and 1956.

Table 1
Statistics for the tree-ring based reconstruction procedures (1981–2001).

	Annual	Seasonal (May ~ October)
r	0.710	0.542
R^2	0.504	0.294
$_{\text{adjusted}}R^2$	0.466	0.255
F	13.201	7.506
P	0.003	0.013
N	17	20
Models[a]	NDVI = 0.105 TRW + 0.150	NDVI = 0.223 TRW + 0.200

[a] *TRW* indicates tree-ring width parameters.

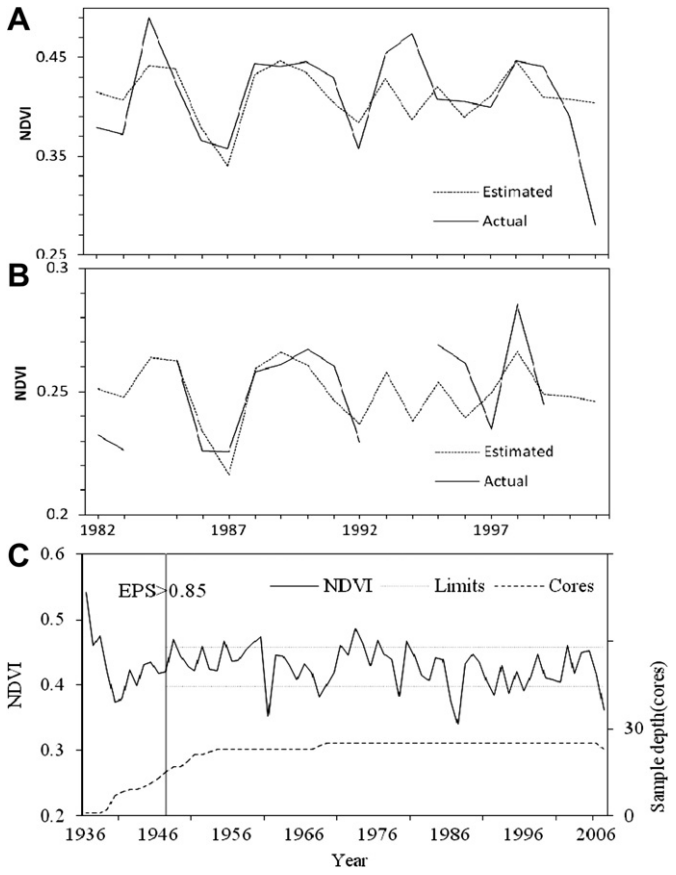

Fig. 2. Comparison of actual (solid) and tree-ring based estimation (dashed) of NDVI for (A) May–October and (B) the yearly mean from 1981 to 2001; and (C) the estimated May–October NDVI from 1936 to 2008 and the corresponding tree-ring sample depth (cores); the lines of limits indicate the boundary of normal and abnormal vegetation cover change; the vertical line indicates the acceptable (valid) time of tree-ring width chronology for the estimation starts at 1947 (EPS > 0.85).

According to the above defined criterion of vegetation cover, both sparse (<MOM − SD = 0.34) and dense anomalies (>MOM + SD = 0.42) of vegetation cover total 22 years (18.96% of the total), and normal density (seasonal mean NDVI range from 0.34 to 0.42) total 72 years (62.07% of the total) in the whole period. After applying a 10-years low pass filter, the monthly NDVI shows 5–7 relatively dense/sparse periods in growing season from 1891 to 2006. The dense vegetation coverage is seen from 1891 to 1910, 1928–1932, 1940–1945, 1953–1963, 1973–1978 and 1985–1998, and sparse coverage is found in 1911–1927, 1933–1939, 1946–1952, 1964–1972, 1979–1984 and 1999–2005. The 1890s, 1900s, 1960s, 1980s, 1990s and 2000s were the dominant dense NDVI decades (seasonal mean NDVI > 0.378), and the 1910s, 1920s 1930s, 1940s, 1950s and 1970s were the dominant sparse NDVI decades (seasonal mean NDVI < 0.378). The mean NDVI for the first half of the 20th century is 0.368, which is lower than the second half of the 20th century mean (0.384) and the full period mean (0.378) by ~2.7% and ~4.4% higher, respectively.

MTM spectral analysis over the full range of our reconstruction revealed some significant cycles at 95% of confidence level. The 2–8 year cycles are significant during the whole period (Appendix Table 2). Seasonally significant spectral peaks are found at 2.2, 2.5, 3.7, 3.8, 4.0–4.6, 4.8, 4.9, 6.1, 6.2, 6.7–7.9, and 8.0–8.2 year cycle, while longer term cycles are also not found (Appendix Table 2).

3.5. Linkages to Asian monsoon and Pacific Ocean activities

Similar patterns were found between our reconstruction and other geophysical processes. The East Asian monsoon system (Shi and Zhu, 2000), as well as the Western North Pacific monsoon system (Wang et al., 1999, 2001), have an obvious effect on regional vegetation cover change and other environmental condition of the steppe through their influence on local climate, especially the summer East Asian monsoon in May and June ($p < 0.05$).

Furthermore, teleconnections were also found between regional vegetation changes and the tropical Pacific Ocean. Signals of ENSO were detected in regional vegetation cover change during the common period ($p < 0.05$), as suggested by the cyclic patterns of 2–4 years and 6–8 years (Allan et al., 1996) (Appendix Table 2), as well as the Tropical Biennial Oscillation (TBO) (Meehl, 1987). The western Pacific Ocean variation has a relatively obvious relationship with the vegetation cover in the growing season, especially in July, August and September ($r = 0.250$, $p = 0.06$). Interestingly, significant correlations have also been observed between the yearly typhoons that hit China ($p < 0.05$) [(Wang et al., 1999), records from 1998 to 2006 were obtained from the Yearly Report on the State of Environment in China], particularly in May and June ($p < 0.01$) during the recent century (1891–2006). In addition, significant correlations between the Arctic Oscillation (AO) and regional vegetation cover were also found, especially during the early spring (May) and late autumn (October) ($p < 0.05$), suggesting an influence of the Arctic climate on the vegetation related environmental change in China's high latitude semi-arid and arid region.

Table 2
Statistics for the PDSI based reconstruction procedures (1981–2001). A) For the reconstruction models, and B) for the regression models of the interpolated values.[a]

A	May			Jun			Jul		Aug		Sep	Oct
Independent	p. July–May	p. Jul–p. Dec	Jan–May	p. Jul–Jun	p. Jul–p. Dec	Jan–Jun	p. Jul–Jul	Jul	Jun–Aug	Jul–Aug	Jul–Sep	Jul–Oct
r	0.916	0.88	0.814	0.911	0.823	0.837	0.665	0.515	0.679	0.653	0.615	0.823
R^2	0.840	0.774	0.663	0.829	0.678	0.701	0.442	0.265	0.461	0.427	0.378	0.677
$_{adjusted}R^2$	0.629	0.669	0.543	0.537	0.529	0.563	−0.594	0.226	0.366	0.363	0.269	0.591
F	3.811	7.410	5.510	2.835	4.556	5.072	0.427	6.855	4.847	6.705	3.450	7.870
P	0.034	0.001	0.005	0.087	0.011	0.007	0.912	0.017	0.013	0.007	0.04	0.001
B	Time											
R^2	1897						0.270		0.234		0.300	0.264
	1898	0.187			0.253		0.270		0.234		0.300	0.264
($R^2 \geq 0.07$,	1899	0.187			0.253		0.270		0.234		0.300	0.264
$P < 0.05$)	1905						0.270		0.234		0.300	0.264
	1944						0.022		0.009		0.114	0.135
	2006						0.172		0.147		0.203	0.214

[a] "p." denotes the prior year. June, July, August, September and October are indicated by Jun, Jul, Aug, Sep and Oct, respectively.

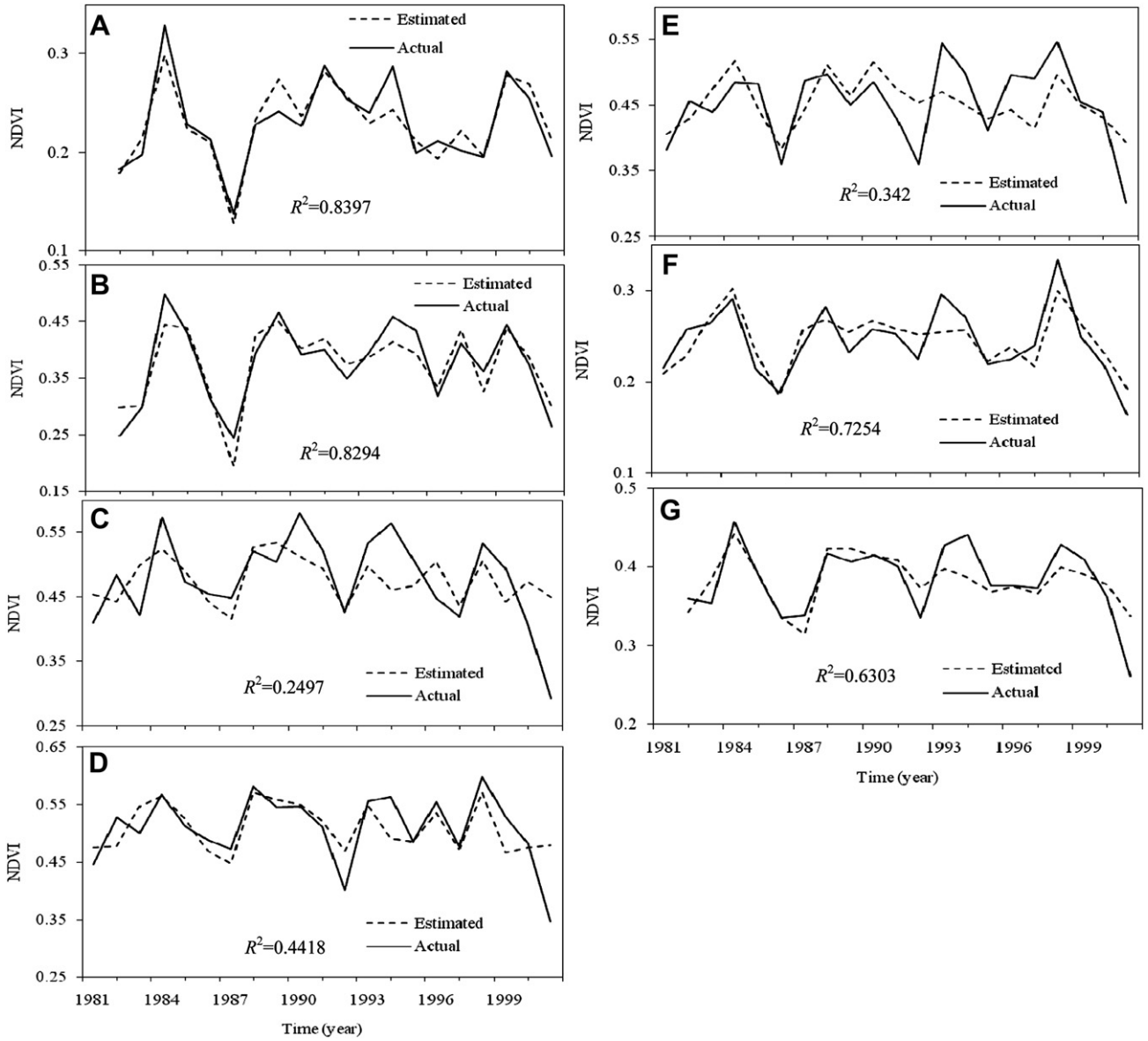

Fig. 3. Comparison of actual (solid) and PDSI based estimation (dashed) of NDVI for May, June (Jun), July (Jul), August (Aug), September (Sep) and October (Oct) and their mean (MEAN) from 1981 to 2001 (A, B, C, D, E, F and G, respectively).

4. Discussion

4.1. Greenness – climate response

Similar to many other climate – vegetation greenness responses in semi-arid or arid areas of northeastern to northwestern China (He and Shao, 2006; Liang et al., 2005), vegetation from the high latitude semi-arid steppe is very sensitive to moisture deficiency and temperature anomalies, especially during the previous growing season to the current growing season (previous July–June) (Appendix Fig. 3). Water availability in this cold semi-arid and arid region is related to thawing soil and melting snowpack, which are partly influenced by previous late-summer/autumn rainfall (August–September) and water storage in the soil during the following winter (October–April). Autumn–winter precipitation/snow (August–April) enriches soil moisture storage and reduces the impacts of a higher water loss through evaporation. Whereas precipitation during the current growing season directly increases soil moisture availability and thus compensates the soil water loss due to evapotranspiration.

According to Liang et al. (2005) monthly precipitation from the previous summer to current autumn shows the greatest impacts on the local semi-arid and arid vegetation cover. Positive correlations found between NDVI and precipitation, together with the negative correlations with temperature, suggest that local vegetation is moisture limited in our study site. The negative response of vegetation cover to temperature indicates that high temperature may indirectly limit plant growth by accelerating evapotranspiration. The strong restraining effects of temperature on vegetation cover during most of the previous and current growing season supports the Kaufmann et al. (2004) study showing that NDVI proxies are indicators of the physiological status of plants. Recent significant increases in annual mean temperature (0.05 °C/year) and the associated increase in evapotranspiration, and a decrease in rainfall (e.g. from ~275 mm in the starting decade of local meteorological records, 1959–1968, to ~214 mm in the ending decade of local meteorological records, 1999–2008) have resulted in severe decreases in vegetation cover and a transition from semi-arid (500 mm > annual rainfall > 250 mm) to arid climate conditions

(annual rainfall < 250 mm). However, there are also positive effects of warmer temperature on vegetation cover during the cold season, and those effects can benefit vegetation vigor in the following growing season. This is consistent with research on climate-vegetation responses in cold regions by Shultz and Halpert (1993).

High, coherent and stable correlations were observed between NDVI and PDSI, particularly from previous July to the current growing season (Table 2; Fig. 1B). This appears to be a common feature of the monthly greenness–climate relationship on the grassland in semi-arid and arid regions of northern China, suggesting that individual months are more important than annual or seasonal conditions regarding vegetation dynamics. The importance of January–July precipitation for community biomass productions in the nearby semi-arid and arid steppe has already been documented in previous studies (Bai et al., 2004). In addition, the significant linkage between NDVI and Mongolian pine tree-ring width in this semi-arid and arid area is due to the common phenological process and the influence of seasonal moisture on these two distinct vegetation types.

4.2. Comparison with regional records

Because the tree-ring based reconstruction and PDSI based estimation show high coherency, our discussion of vegetation dynamics will focus on the longer PDSI based estimation. The correlation analysis suggests that our reconstruction is representative of the regional vegetation variability at the Hulunbei'er steppe. Therefore, our reconstruction provides valuable environmental information for this semi-arid and arid region.

Our reconstruction preserves the inter-monthly and inter-decadal vegetation variability (Appendix Table 2; Fig. 4). Although no significant cycles above 10-years were detected, there is a low-frequency decreasing processes on the vegetation cover, which indicates a significant desertification process occurring on this fragile semi-arid and arid steppe during the 20th century. The decreasing NDVI over the past few decades is linked to a warmer Northern China—a parameter that might help improve efforts to predict how vegetation cover in semi-arid and arid area will behave in a warming world. The lengths of 1891–1952 and 1953–2006, the two semi-century-long decreasing processes were 61 years and 53 years respectively. The former has a decreasing rate of 0.27% per year and the latter has decreased by 0.29% per year on average. During the two periods of decreasing NDVI (1891–1952 and 1953–2006), low moisture was also detected in tree rings on the west side of the semi-arid and arid steppe in Northeast and West-Central Mongolia (Davi et al., 2006; Pederson et al., 2001). The recent rapid decrease of PDSI and shrinkage of Hulun Lake [decreasing at a mean speed of 0.14 m/year (ranging from 0.08 m/year to 0.67 m/year) during recent two decades (http://www.pecad.fas.usda.gov/rssiws/images/lakes/lake0385.TPJO.1.txt)] verifies the decrease of regional vegetation cover and the degradation of the semi-arid and arid environment.

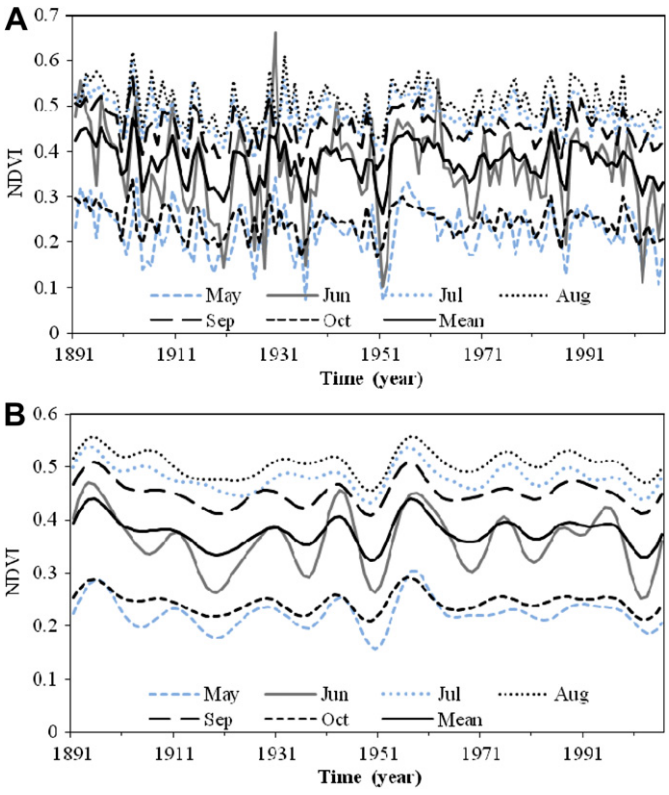

Fig. 4. (A) PDSI based estimation of NDVI for May, June (Jun), July (Jul), August (Aug), September (Sep) and October (Oct) and their mean from 1891 to 2001; and (B) their 10-year low pass filter.

Local vegetation cover anomalies may indicate some complex environmental and ecological events at a large scale, such as dust storms and locust plagues (*Locusta migratoria manilensis*) across China. For example, the droughts and strong dust storms documented in 1900 and 1901, suggested by previous studies (Deng and Jiang, 2006), match with the two sparse vegetation cover years in our reconstruction. The very severe locust plagues (Wu et al., 2006) across China in 1951 and 1952 occurred during the two most sparsely covered vegetation years. Furthermore, 55% of the dust records (6/11), named "Yutu" from 1891 to 1935 (Zhang, 1982) agreed with our estimates of sparse vegetation cover at a seasonal level (averaged May–October), the percentage of correspondence with monthly sparse vegetation cover is 73% (8/11) in May and June. This suggests that the vegetation cover is more important in the semi-arid and arid steppe during the spring.

4.3. Verification of regional characteristics

There are no long-term vegetation cover records, and few reported vegetation cover time series are available in China. The local dryness/wetness and proxies such as tree rings can be used to indicate and estimate typical grassland NDVI variability in northern China (He and Shao, 2006; Liang et al., 2005, 2009). NDVI is also a very good indicator of drought in arid environments. Here, regional climate and tree-ring data were used to verify the sparse/dense vegetation conditions of semi-arid and arid steppe at large scales. The vegetation cover in the first half of the 20th century was sparse, and associated with relatively dry conditions in Northwest China, Mongolia and Northeast China (Chen et al., 2011; Davi et al., 2006; He and Shao, 2006; Liang et al., 2009; Pederson et al., 2001). At inter-annual and decadal scales, some severely sparse (dry) or dense (wet) periods, like the 1920s and 1953–1963 were recorded in other tree-ring studies (He and Shao, 2006), and clearly detected in our work (Fig. 4). Our actual and estimated data demonstrated that the sustained droughts in 1983–1989 and 2000–2001 suppressed the growth of trees and grass, whereas in the 1990s the increment in precipitation favored both, tree and grass growth (Liang et al., 2009).

In conclusion, the estimated century-long records from trees and climate show that vegetation cover in semi-arid and arid steppe regions of northern China have highly variability through sparse and dense variation in space and time. This variability (sparse and dense) reflects regional dynamics of vegetation cover as well as the regional semi-arid environmental variation (e.g. dust storms occurrence, insects, lake shrinkage, etc), and a possible link between the Arctic and Pacific Ocean climate activities and climate

warming. This study demonstrates that climate variability is linked to grassland productivity in the semi-arid regions of China (through NDVI) and changes in climate (as seen in the instrumental record), particularly warming and drying (in addition to changes in agricultural practices), can exacerbate degradation and desertification, and the ability of the grassland to support grazing.

Acknowledgments

This work was funded by the National Natural Science Foundation of China Project 41071035, 31100327, 30600093, 31000222, 31000225 and 90411019, and China Special Research Program for Public-Welfare Forestry (Grant No. 200804001). We would like to thank Dr. Hui Deng for dust storm data. We also thank Ms. Jieping Liu and Dr. Laia Andreu for their helpful work.

Appendix A. Supplementary material

Supplementary data related to this article can be found online at doi:10.1016/j.jaridenv.2012.03.013.

References

Allan, R., Lindesay, J., Parker, D., 1996. El Niño–Southern Oscillation and Climatic Variability. Commonwealth CSIRO Publishing, Australia, 405 pp.
Bai, Y., Han, X., Wu, J., Chen, Z., Li, L., 2004. Ecosystem stability and compensatory effects in the Inner Mongolia grassland. Nature 431, 181–184.
Blasing, T.J., Duvick, D.N., West, D.C., 1981. Calibration and verification using regionally averaged single station precipitation data. Tree-Ring Bulletin 41, 37–44.
Chen, M., Xie, P., Janowiak, J.E., Arkin, P.A., 2002. Global land precipitation: a 50-yr monthly analysis based on gauge observations. Journal of Hydrometeorology 3, 249–266.
Chen, Z., He, X., Cook, E.R., He, H.-S., Chen, W., Sun, Y., Cui, M., 2011. Detecting dryness and wetness signals from tree rings in Shenyang, Northeast China. Palaeogeography, Palaeoclimatology, Palaeoecology 302, 301–310.
Cook, E.R., 1985. A time-series analysis approach to tree-ring standardization. PhD dissertation, The University of Arizona, Tucson.
Cook, E.R., Holmes, R.L., 1986. Users manual for program ARSTAN. In: Holmes, R.L., Adams, R.K., Fritts, H.C. (Eds.), Tree-ring Chronologies of Western North America: California, Eastern Oregon and Northern Great Basin. CHRONOLOGYSER. 6. The University of Arizona, Tucson, pp. 50–65.
Cook, E.R., Meko, D.M., Stahle, D.W., Cleaveland, M.K., 1999. Drought reconstructions for the continental United States. Journal of Climate 12, 1145–1162.
Dai, A., Fung, I., Del Genio, A.D., 1997. Surface observed global land precipitation variations during 1900-1988. Journal of Climate 10, 2943–2962.
Dai, A., Trenberth, K.E., Qian, T., 2004. A global data set of Palmer Drought Severity Index for 1870–2002: relationship with soil moisture and effects of surface warming. Journal of Hydrometeorology 5, 1117–1130.
Davi, N.K., Jacoby, G.C., Curtis, A.E., Baatarbileg, N., 2006. Extension of drought records for central Asia using tree rings: West-Central Mongolia. Journal of Climate 19, 288–299.
Deng, H., Jiang, W.F., 2006. Temporal-spatial distribution and characteristics of the sand-dust weathers in North China Plain from 1463 to 1913. Progress in Natural Science 16 (5), 596–603 (in Chinese).
Fabricante, I., Oesterheld, M., Paruelo, J.M., 2009. Annual and seasonal variation of NDVI explained by current and previous precipitation across Northern Patagonia. Journal of Arid Environments 73, 745–753.
Fang, J., Piao, S., Zhou, L., He, J., Wei, F., Myneni, R.B., Tucker, C.J., Tan, K., 2005. Precipitation patterns alter growth of temperate vegetation. Geophysical Research Letters 32, L21411.
Fritts, H.C., 1976. Tree Rings and Climate. Academic Press, London.
Han, L.-C., 2001. A method of modifying error for non-synchronicity of grass yield remote sensing estimation and measurement. International Journal of Remote Sensing 22 (17), 3363–3372.
He, J., Shao, X., 2006. Relationships between tree-ring width index and NDVI of grassland in Delingha. Chinese Science Bulletin 51 (9), 1106–1114.
Holmes, R.L., 1983. Computer-assisted quality control in tree-ring dating and measurement. Tree-Ring Bulletin 43, 69–95.
Jiang, G.M., Han, X.G., Wu, J.G., 2006. Restoration and management of the Inner Mongolia grassland require a sustainable strategy. Ambio 35, 269–270.
Jones, P.D., Moberg, A., 2003. Hemispheric and large-scale surface air temperature variations: an extensive revision and an update to 2001. Journal of Climate 16, 206–223.
Kaufmann, R.K., D'Arrigo, R.D., Laskowski, C., Myneni, R.L., Zhou, B., Davi, N.K., 2004. The effect of growing season and summer greenness on northern forests. Geophysical Research Letters 31, L09205. doi:10.1029/2004GL019608.
Li, B., 1999. Genera characters of steppe of China. In: Editorial Committee (Ed.), Collection of Li Bo. Science Press, Beijing (in Chinese).
Liang, E., Eckstein, D., Liu, H., 2009. Assessing the recent grassland greening trend in a long-term context based on tree-ring analysis: a case study in North China. Ecological Indicators 9, 1280–1283.
Liang, E.Y., Shao, X.M., He, J.C., 2005. Relationships between tree growth and NDVI of grassland in the semiarid grassland of north China. International Journal of Remote Sensing 26 (13), 2901–2908.
Ma, W.H., Yang, Y.H., He, J.S., Zeng, H., Fang, J.Y., 2008. Above- and belowground biomass in relation to environmental factors in temperate grasslands, Inner Mongolia. Science in China (Seriers C-Life Sciences) 51 (3), 263–270.
Mann, M.E., Lee, J.M., 1996. Robust estimation of background noise and signal detection in climatic time series. Climatic Change 33, 409–445.
Meehl, G.A., 1987. The annual cycle and interannual variability in the tropical Pacific and Indian Ocean region. Monthly Weather Review 115, 27–50.
Palmer, W.C., 1965. Meteorological Drought. Res. Paper No. 45. Dept. of Commerce, Washington, D.C, 58 pp.
Pederson, N., Jacoby, G.C., D'Arrigo, R., Cook, E.R., Buckley, B.M., Dugarjav, C., Mijiddorj, R., 2001. Hydrometeorological reconstructions for northeastern Mongolia derived from tree rings: AD 1651–1995. Journal of Climate 14, 872–881.
Schultz, P.A., Halpert, M.S., 1993. Global correlation of temperature, NDVI and precipitation. Advance in Space Research 13 (5), 277–280.
Scurlock, J.M.O., Johnson, K., Olson, R.J., 2002. Estimating net primary productivity from grassland biomass dynamics measurements. Global Change Biology 8 (8), 736–753.
Shi, N., Zhu, Q.G., 2000. The East Asia summer/winter monsoon index for 1873–1996. Meteorological Science and Technology 3, 14–18 (in Chinese).
Stokes, M.A., Smiley, T.L., 1968. An Introduction to Tree-Ring Dating. The University of Chicago Press, Chicago.
Tucker, C.J., 1979. Red and photographic infrared linear combinations for monitoring vegetation. Remote Sensing of Environment 8 (2), 127–150.
Tucker, C.J., Pinzon, J.E., Brown, M.E., 2004. Global Inventory Modeling and Mapping Studies. NA94apr15b.n11-VIg, 2.0, Global Land Cover Facility. University of Maryland, College Park, Maryland. 04/15/1994.
Tucker, C.J., Sellers, P.J., 1986. Satellite remote sensing of primary production. International Journal of Remote Sensing 7, 1395–1416.
Wang, B., Wu, R., Lau, K.-M., 2001. Interannual variability of Asian summer monsoon: contrast between the Indian and Western North Pacific–East Asian monsoons. Journal of Climate 14, 4073–4090.
Wang, J., Rich, P.M., Price, K.P., Kettle, W.D., 2004. Relations between NDVI and tree productivity in the central Great Plains. International Journal of Remote Sensing 25, 3127–3138.
Wang, R.Z., 2004. Photosynthetic pathways and life form types for native plant species from Hulunbeier Rangelands, Inner Mongolia, North China. Photosynthetica 42 (2), 219–227.
Wang, S.W., Gong, D.Y., Chen, Z.H., 1999. Serious climatic disasters of China during the past 100 years. Quarterly Journal of Applied Meteorology 10 (Supp), 43–53 (in Chinese).
Wigley, T., Briffa, K.R., Jones, P.D., 1984. On the average value of correlated time series, with applications in dendroclimatology and hydrometeorology. Journal of Climate and Applied Meteorology 23, 201–213.
Wu, R.F., Huo, Z.G., Lu, Z.G., 2006. Climatological cause and long-term prediction of occurrence of East Asia migratory locusts in China. Journal of Natural Disasters 15 (4), 71–78 (in Chinese).
Yang, G., Chen, X., Zhou, D., 1992. Ordination and gradient analysis of coniferous forest in Daxinganling. Journal of Northeast Forestry University 3 (1), 42–47.
Yi, B.Z., 2003. Exploitation of Chinese northeast grasslands and its cost at ecological environment since the Qing dynasty. Agricultural History of China 4, 112–119 (in Chinese).
Zhang, D., 1982. Analysis on the phenomena of "Yutu" in historical times. Chinese Science Bulletin 5, 294–297.
Zhang, Z.T., Liu, Q., 1992. Rangeland Resources of the Main Pasture Areas in China and Their Development and Utilization. China Science and Technology Press, Beijing (in Chinese).